PCCP

Accepted Manuscript

ROYAL SOCIETY OF CHEMISTRY

www.rsc.org/pccp

PCCP RSCPublishing

COMMUNICATION

Preference for Propellane motif in Pure Silicon Nanosheets

Cite this: DOI: 10.1039/x0xx00000x

S. Marutheesswaran[a], Pattath D. Pancharatna[a] and Musiri M. Balakrishnarajan*[a]

Received 00th March 2013,
Accepted 00th March 2013

DOI: 10.1039/x0xx00000x

www.rsc.org/

Free standing silicene nanosheets remain elusive presumably due to the instability associated with sp^2 hybridized silicon atoms. Here we show that silicon prefers nanosheets based on the non-classical Si_5 with [1.1.1]-propellane motif that has two inverted tetrahedral atoms bridged by three tetrahedral atoms. DFT calculations show that nanosheets constructed exclusively from propellane building blocks are consistently more stable than those with sp^2 silicon atoms or their hybrids. These nanosheets also exhibit a narrow but definite band gap, unlike those reported earlier.

Contrary to carbon, silicon seldom prefers π-bonding primarily due to the large difference in the diffuseness of its 3s and 3p orbitals, despite their energetic proximity[1]. The inherent poor π-overlap[2] weakens π-bond strength in Si (25 kcalmol^{-1}) compared to carbon (75 kcalmol^{-1}). Obviously, unsaturated Si systems are highly reactive, relatively rare[2-4] and also exhibit out-of-plane distortion. The stabilizing effects of similar organic systems like conjugation and aromaticity are virtually non-existent for silicon. The only conjugated system known with Si is the butadiene analogue and is non-planar.[5] For the benzene analogue[6], calculations show that Si_6H_6 (D_{6h}) undergoes D_{3d} distortion[7] and even this distorted geometry is less stable than several other structures[8]. The only structure with a cyclic Si_6 skeleton isolated experimentally, termed 'dismutationally aromatic', has tetrahedral atoms[9]. DFT calculations on silicene indicates its tendency for D_{3d}-distortion[10] , but this free standing all-silicon nanosheets still elude experimental characterization. Though there are reports on the possible existence of distorted silicene on metal surfaces[11], they are unstable without the metal support[12-14] and collapse irreversibly to the near sp^3 hybridized bulk structure over time[12]. These observations show that stable nanosheets with sp^2-silicon is unlikely, distorted or otherwise[15]. Looking for alternatives, here we explore the possibility of 2D-nanosystems that are energetically more preferred over the sp^2 hybridized silicene.

Truncating the third dimension without π-bonding in all silicon network necessitates non-classical bonding. Both theory and experiments show that silicon has the propensity to form [1.1.1]-propellane framework with a Si_5 trigonal bipyramidal geometry (*tbp*), which has two inverted tetrahedral bridge-heads(Si_{bh}) linked through three sp^3 Si bridges(Si_b)[16]. Apart from its experimental characterization[17], the global minimum of Si_6H_6 is computed to have this *tbp* framework with an additional tetrahedral Si connecting two of the bridges that is ~50kcal/mol more stable than the cyclic Si_6H_6 (D3d)[8]. Such a bridged propellane structure[9,18] is also formed by the thermal rearrangement of the cyclic Si_6 structure[19]. Further, DFT assessment of the adatom preferences on silicene[20] and exploration of energetic preferences of different surfaces peeled off from bulk silicon[21], both show *tbp* units on geometry optimization. These observations motivated us to inquire on *tbp* framework as a potential building block for silicon-based 2D-nanosystems

The *tbp* geometry of propellane (D_{3h}), with its six exo-bonds, offers an array of isomeric possibilities (Fig 1). The adjacent *tbp* units can be connected along the C2 axis in two ways: (i) the '*tail-to-head*' form in which two Si_b atoms of a *tbp* unit connect to the same Si_b atom of its neighbour, preserving the mirror plane along the translation direction (ii) the '*tail-to-tail*' form in which two Si_b atoms of a *tbp* unit connect to two distinct Si_b atoms of its adjacent *tbp* unit. These two topologies lead to distinct one dimensional chains in which the Si_{bh} lies in a linear and zig-zag arrangement. The linear chain can be stacked to form 2D-sheets where the Si_{bh} of the adjacent chains are either *cis* or *trans* with respect to each other. The *cis* structure has a rectangular lattice with *Pm* space symmetry and has only one *tbp* fragment per unit cell. The *trans* isomer falls in a higher *P2mg* space symmetry, with two *tbp* per unit cell which are related by a C_2 axis at the lattice centre and a gliding plane containing this C_2.

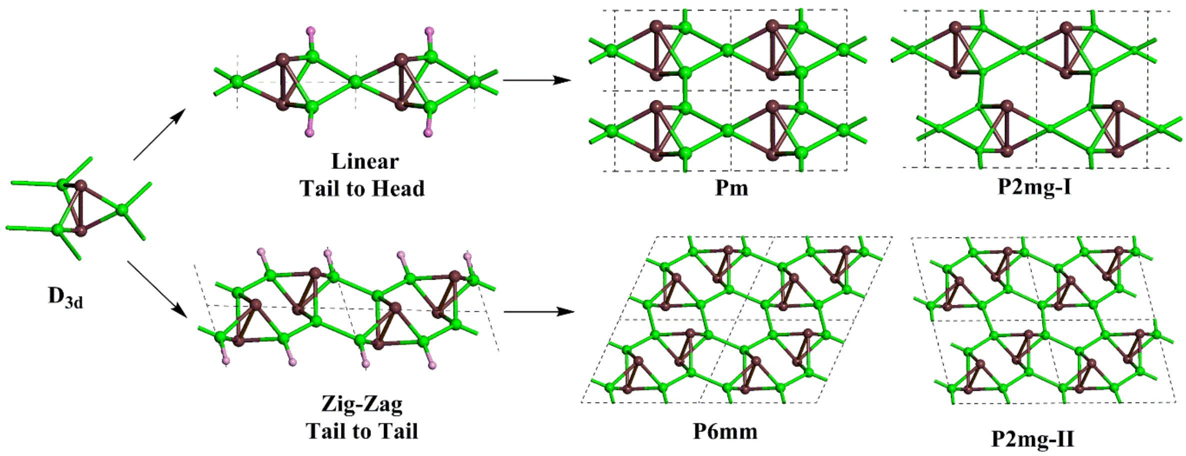

Fig.1 Schematic illustration of the distinct ways of connecting adjacent propellane units to form 1D chains and 2D-sheets. The bridgeheads and bridges are coloured differently for clarity.

Likewise, stacking of the zig-zag chain leads to two isomeric sheets; another *P2mg* structure (*P2mg-II*) that has AA type stacking and a hexagonal structure with a high *P6mm* space symmetry, formed from AB type stacking. In both these isomers, there are two propellane units per unit cell that are related by a C2 axis and a mirror plane.

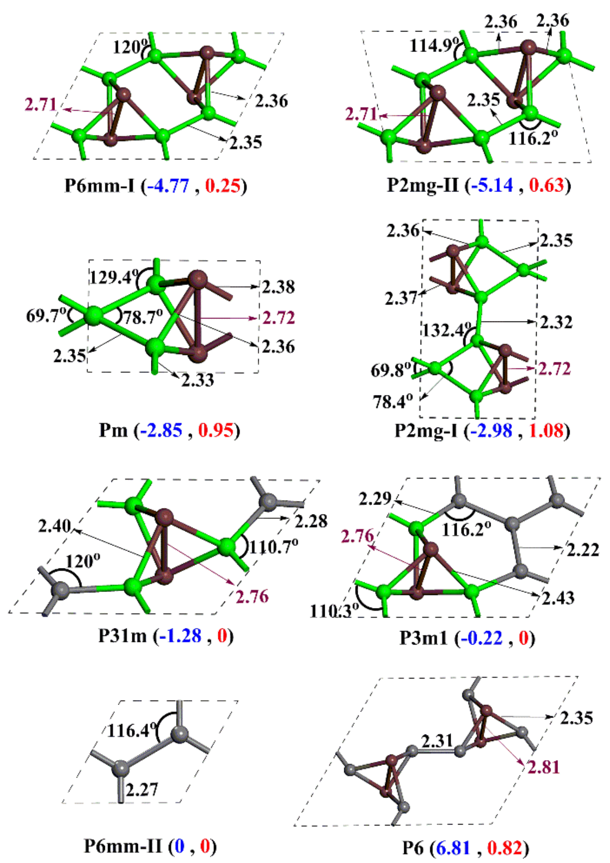

Fig. 2 Optimized geometrical parameters of various 2D-Silicon nanosheets along with relative energies (kcal/mol) per Si atom and band gaps (eV) within brackets.

DFT calculations on these four 2D-nanostructures with full optimization of the unit cell parameters and ionic positions within the lattice symmetry constraints show that all of them are energetically more preferred than the D_{3d} distorted silicene nanosheets (Fig 2). The propellane isomer *P2mg-II* is more stable than silicene by 5.14 kcal/mol of Si atom, *which is* closely followed by the hexagonal *P6mm-I* isomer. The *P2mg-I* and *Pm* structures are ~3 kcal/mol more stable than silicene. The various Si-Si bond distances show little variation among all these isomers. The Si_b-Si_{bh} bond lengths are in the range of 2.36Å – 2.38Å, while the Si_b-Si_b bonds are 2.32Å- 2.35Å, comparable to the Si-Si single bond length of 2.351Å in bulk silicon. The bond between the inverted tetrahedral atoms are in the range of 2.71Å -2.72Å, longer than the experimental bond length (2.638Å) in the silicon propellane that has mesityl substituents[17] but comparable to that of the isolated Si_6R_6 molecule[9]. Since Si-Si distances hardly vary across isomers, we focussed on the angle strain around Si_b atoms to explain their relative stability. The internal Si_{bh}-Si_b-Si_{bh} angle vary little across isomers (~70˚) since the Si_{bh}-Si_{bh} distances are nearly equal but significant variations are observed between the exo-bonds of Si_b. Compared to the near tetrahedral H-Si-H angle (110˚) in the computed *tbp* geometry[16] of Si_5H_6, the most stable *P2mg-II* isomer exhibits only slight deviations (5˚ and 7˚) in two different bridges. The next stable *P6mm* isomer has a comparatively larger deviation of 120˚, constrained by hexagonal symmetry. However, the isomers *P2mg-I* and *Pm* constructed from linear chains have an acute angle (~78˚) in one of its bridges while the other two bridges have obtuse angles (129˚) enforced primarily by their topology. These deviations correlate very well with the observed stability ordering among these isomers.

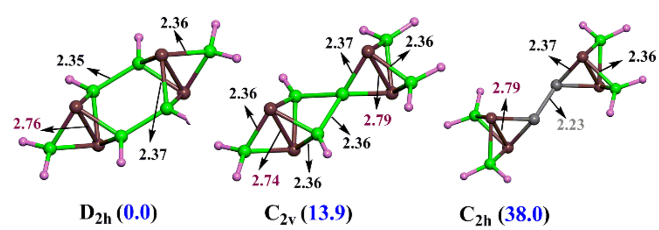

Fig. 3 The optimized geometry of propellane dimers connected tail-to-tail (D2h), tail-to-head (C2v) and head-to-head (C_{2h}) and their relative energies (kcal/mol).

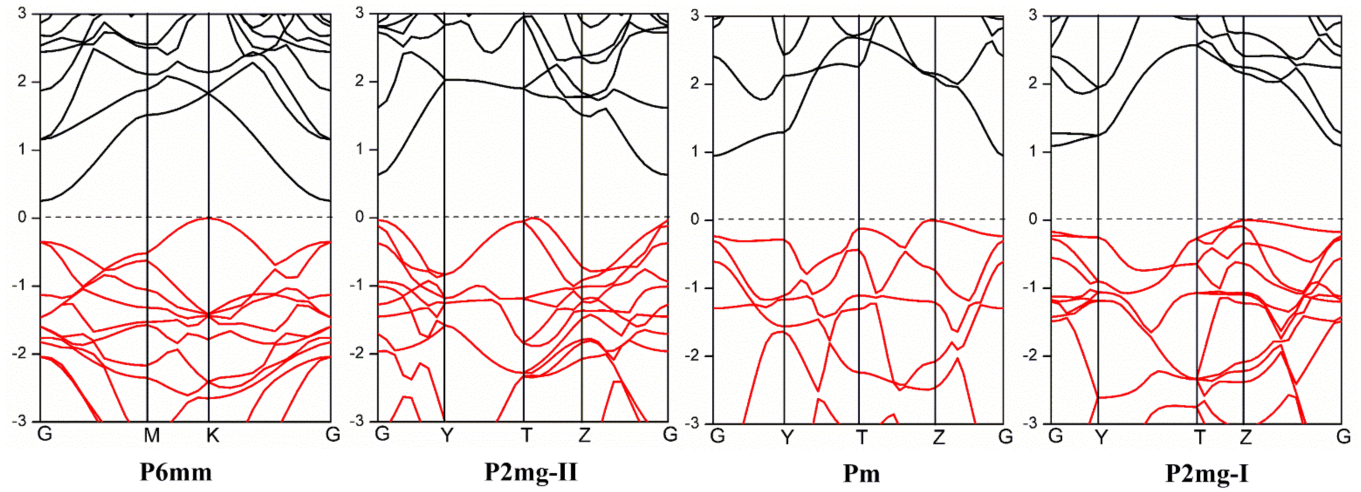

Fig. 4 The DFT computed band structures of the four propellane based 2D-silicon nanosystems.

To ascertain that the enforced symmetry of various 2D-sheets is free from further distortion, molecular calculations are also done on possible *tbp* dimers. The pendent bonds are terminated with hydrogen atoms to generate three $Si_{10}H_8$ isomers (Fig 3). Molecular DFT calculations characterize all these structures as minimum on their potential energy surface, and the 'tail-to-tail' isomer is found to be more stable than the 'head-to-tail' isomer. The isomer linked by a double bond ('head-to-head') is the least stable as expected.

The computed band-structure of the 2-D sheets using DFT (Fig 4) show that all are narrow band-gap semiconductors unlike silicene which is metallic even with the D_{3d} distortion. However, there is no correlation between total energy and band-gap among these isomers. Isomers *Pm* and *P2mg-I* that are constructed from linear chain has a larger gap compared to the more stable zig-zag chain based isomers *P2mg-II* and *P6mm*. The valence band maximum occurs at K for the *P6mm* isomer and between T and Z in rectangular lattices. The conduction band minimum is always at G for all the isomers, displaying indirect band gap. The variation in band gap is primarily caused by the width of the conduction band. In rectangular lattices, the degeneracy of the topmost valence band at G is lost and one of the split-off band has the same symmetry with the conduction band. Mixing of these two bands leads to avoided crossing that increases the band-gap. In the highly symmetric *P6mm* isomer, such a mixing is absent which presumably increases the width of the conduction band. A comparison of bond-distances with band gap shows that the distance between adjacent *tbp* units correlates well with the band gap. (See supplementary information (SI) for bonding details of the frontier bands Figs S1-S2).

Since the width of the conduction band and consequently band gap is directly proportional to the interaction between the Si_b atoms of the adjacent *tbp* units, we anticipated that separating the *tbp* units by spacers constructed from sp^2 silicon will increase the band gap further. Unfortunately, hexagonal sheets with spacers (Fig 2) like single sp^2 silicon atom (*P31m*) and a D3d symmetric analogue of tetramethylene methane (*P3m1*) are reported to be metallic. Our calculations show that these lattices are less stable compared to all the pure *tbp* sheets though more stable than silicene. Suspecting the disjoint sp^2 Si radical spacers as the probable cause for metallicity, we also optimized the hexagonal *P6* isomer (Fig 2) that has localized double bonds between Si_b atoms of the adjacent *tbp* units ('head-to-head'). The planarity was not enforced around the Si_b atoms as its molecular analogue shows pyramidalization around Si_b atoms (Fig 3 C). The resulting structure has finite band gap as expected (see SI, Fig S3). However, despite the pyramidalization of the Si_b atoms away from its bonded neighbours (0.41 Å) it is less stable even compared to silicene as the energetically preferred sp^3 hybridized atoms of *tbp* is replaced by the unfavourable sp^2 hybridization. Our attempts to increase the band gap by introducing other sp^2 hybridized silicon spacers between *tbp* units that allows double bond localization within their framework proved futile as they are all found to be metallic (See SI, Fig S4).

The consistent high stability of all the propellane based nano-sheets compared to silicene indicates that the instability associated with the delocalized π-bonding in silicene far outweighs the destabilization arising from the inverted tetrahedral geometry of the Si_{bh} despite their long and weak bonds. Considering that DFT calculations with GGA functionals are typically known to underestimate the band-gap, the observation of finite band-gap for all these isomeric silicon sheets based on pure *tbp* motif is truly remarkable and has strong implications in semiconductor electronics. We predict that these *tbp* based nanosheets will be preferentially formed by bottom-up approaches even in the absence of metal support since they are inherently more stable and also can be synthesized from molecular propellane derivatives with labile substituents by controlled polymerization. Our calculations clearly shows that sp^2 silicon atoms are detrimental to the stability and leads to metallic character even when embedded in a stable *tbp* sublattice. The propellane motif is also ideal for 2D-nanosystems of other heavier analogues of carbon and their hybrids as they are proved susceptible for oligomerization[22].

Computational Methods:

Calculations on all the nanosheets are performed within the framework of density functional theory (DFT) as implemented in the Cambridge Ab-initio Serial Total energy package (CASTEP), available in the Materials Studio software[23]. We employed non-local corrected generalized gradient approximation[24] based on the Perdew-Burke-Ernzerhof[25] (PBE) formulation along with ultrasoft pseudo potentials with the plane-wave cut-off of 600eV in a Monkhorst-Pack[26] 10x10x1 k-point mesh. The adjacent sheets are kept 25Å away to avoid all possible interactions. The individual atom positions as well as lattice parameters are simultaneously optimized to arrive at the well converged geometries with the chosen cutoff values for energy (10^{-5} eV) and forces (0.01eV). Geometry optimization and vibrational analysis of molecules are done at B3LYP/6-311+G** level of theory using Gaussian 09 package[27].

Acknowledgments

We thank the Department of Science and Technology (DST) New Delhi, for financial support. The DST Young Scientist award to PDP is gratefully acknowledged.

Notes and references

[a] Chemical Information Sciences lab, Department of chemistry, Pondicherry university, Puducherry, 605014. India.

Electronic Supplementary Information (ESI) available: Additional figures showing band structures and MO mapping. Optimised coordinates of 2-D nanosheets and molecules. See DOI: 10.1039/c000000x/

1. W. Kutzelnigg, *Angew. Chem., Int. Ed.*, 1984, **23**, 272.
2. G. Bouhadir and D. Bourissou, *Chem. Soc. Rev.*, 2004, **33**, 210.
3. R. West, M. J. Fink and J. Michl, *Science*, 1981, **214**, 1343.
4. R. C. Fischer and P. P. Power, *Chem. Rev.*, 2010, **110**, 3877; P. P. Power, *Chem. Rev.*, 1999, **99**, 3463.
5. M. Weidenbruch, S. Willms, W. Saak and G. Henkel, *Angew. Chem., Int. Ed.*, 1997, **36**, 2503; M. Ichinohe, K. Sanuki, S. Inoue and A. Sekiguchi, *Organometallics*, 2004, **23**, 3088; M. Ichinohe, K. Sanuki, S. Inoue and A. Sekiguchi, *Silicon Chem.*, 2007, **3**, 111.
6. A. Tsurusaki, C. Iizuka, K. Otsuka and S. Kyushin, *J. Am. Chem. Soc.*, 2013, **135**, 16340.
7. M. Moteki, S. Maeda and K. Ohno, *Organometallics*, 2009, **28**, 2218; K. K. Baldridge, O. Uzan and J. M. L. Martin, *Organometallics*, 2000, **19**, 1477.
8. A. S. Ivanov and A. I. Boldyrev, *J. Phys. Chem. A*, 2012, **116**, 9591.
9. K. Abersfelder, A. J. P. White, H. S. Rzepa and D. Scheschkewitz, *Science*, 2010, **327**, 564.
10. K. Takeda and K. Shiraishi, *Phys. Rev. B*, 1994, **50**, 14916; G. G. Guzmán-Verri and L. C. Lew Yan Voon, *Phys. Rev. B*, 2007, **76**, 075131; S. Cahangirov, M. Topsakal, E. Aktürk, H. Şahin and S. Ciraci, *Phys. Rev. Lett.*, 2009, **102**, 236804; M. Houssa, G. Pourtois, V. V. Afanas'Ev and A. Stesmans, *Appl. Phys. Lett.*, 2010, **97**, 112106; D. Jose and A. Datta, *J. Phys. Chem. C*, 2012, **116**, 24639; D. Jose and A. Datta, *Acc. Chem Res.*, 2013, **47**, 593; A. O'Hare, F. V. Kusmartsev and K. I. Kugel, *Nano Lett.*, 2012, **12**, 1045; E. Cinquanta, E. Scalise, D. Chiappe, C. Grazianetti, B. Van Den Broek, M. Houssa, M. Fanciulli and A. Molle, *J. Phys. Chem. C*, 2013, **117**, 16719; M. Houssa, B. van den Broek, E. Scalise, B. Ealet, G. Pourtois, D. Chiappe, E. Cinquanta, C. Grazianetti, M. Fanciulli, A. Molle, V. V. Afanas'ev and A. Stesmans, *Appl. Surf. Sci.*, 2014, **291**, 98.
11. B. Lalmi, H. Oughaddou, H. Enriquez, A. Kara, S. Vizzini, B. Ealet and B. Aufray, *Appl. Phys. Lett.*, 2010, **97**, 223109; P. Vogt, P. De Padova, C. Quaresima, J. Avila, E. Frantzeskakis, M. C. Asensio, A. Resta, B. Ealet and G. Le Lay, *Phys. Rev. Lett.*, 2012, **108**, 155501; A. Fleurence, R. Friedlein, T. Ozaki, H. Kawai, Y. Wang and Y. Yamada-Takamura, *Phys. Rev. Lett.*, 2012, **108**, 245501; B. Feng, Z. Ding, S. Meng, Y. Yao, X. He, P. Cheng, L. Chen and K. Wu, *Nano Lett.*, 2012, **12**, 3507; C. L. Lin, R. Arafune, K. Kawahara, N. Tsukahara, E. Minamitani, Y. Kim, N. Takagi and M. Kawai, *Appl. Phys. Express*, 2012, **5**, 045802; S. Colonna, G. Serrano, P. Gori, A. Cricenti and F. Ronci, *J. Phys. Condens. Matter*, 2013, **25**, 315301; L. Meng, Y. Wang, L. Zhang, S. Du, R. Wu, L. Li, Y. Zhang, G. Li, H. Zhou, W. A. Hofer and H. J. Gao, *Nano Lett.*, 2013, **13**, 685; T. Morishita, M. J. S. Spencer, S. Kawamoto and I. K. Snook, *J. Phys. Chem. C*, 2013, **117**, 22142.
12. A. Acun, B. Poelsema, H. J. W. Zandvliet and R. Van Gastel, *Appl. Phys. Lett.*, 2013, **103**, 263119.
13. H. Jamgotchian, Y. Colignon, N. Hamzaoui, B. Ealet, J. Y. Hoarau, B. Aufray and J. P. Bibérian, *J. Phys. Condens. Matter*, 2012, **24**, 172001.
14. J. Gao and J. Zhao, *Sci.Rep.*, 2012, **2**:861.
15. E. F. Sheka, *Int. J. Quant. Chem.*, 2013, **113**, 612.
16. D. Nied and F. Breher, *Chem. Soc. Rev.*, 2011, **40**, 3455; T. Iwamoto and S. Ishida, *Chem. Lett.*, 2014, **43**, 164.
17. D. Nied, R. Köppe, W. Klopper, H. Schnöckel and F. Breher, *J. Am. Chem. Soc.*, 2010, **132**, 10264.
18. R. J. F. Berger, H. S. Rzepa and D. Scheschkewitz, *Angew. Chem., Int. Ed.*, 2010, **49**, 10006.
19. K. Abersfelder, A. J. P. White, R. J. F. Berger, H. S. Rzepa and D. Scheschkewitz, *Angew. Chem., Int. Ed.*, 2011, **50**, 7936.
20. V. Ongun Özçelik and S. Ciraci, *J. Phys. Chem. C*, 2013, **117**, 26305.
21. D. Kaltsas and L. Tsetseris, *Phys. Chem. Chem. Phys.*, 2013, **15**, 9710.
22. Y. Ito, V. Y. Lee, H. Gornitzka, C. Goedecke, G. Frenking and A. Sekiguchi, *J. Am. Chem. Soc*., 2013, **135**, 6770.
23. M. D. Segall, J. D. L. Philip, M. J. Probert, C. J. Pickard, P. J. Hasnip, S. J. Clark and M. C. Payne, *J. Phys. Condens. Matter*, 2002, **14**, 2717.
24. J. P. Perdew and Y. Wang, *Phys. Rev. B* 1992**, 45** (23), 13244.
25. J. P. Perdew, K. Burke and M. Ernzerhof, *Phys. Rev. Lett.*, 1996**, 77** (18), 3865.
26. H. J. Monkhorst and J. D. Pack, *Phys. Rev. B* 1976**, 13** (12), 5188.
27. Gaussian 09, Revision A.02, M. J. Frisch, G. W. Trucks, H. B. Schlegel, G. E. Scuseria, M. A. Robb, J. R. Cheeseman, G. Scalmani, V. Barone, B. Mennucci, G. A. Petersson, H. Nakatsuji, M. Caricato, X. Li, H. P. Hratchian, A. F. Izmaylov, J. Bloino, G. Zheng, J. L. Sonnenberg, M. Hada, M. Ehara, K. Toyota, R. Fukuda, J. Hasegawa, M. Ishida, T. Nakajima, Y. Honda, O. Kitao, H. Nakai, T. Vreven, J. A. Montgomery, Jr., J. E. Peralta, F. Ogliaro, M. Bearpark, J. J. Heyd, E. Brothers, K. N. Kudin, V. N. Staroverov, R. Kobayashi, J. Normand, K. Raghavachari, A. Rendell, J. C. Burant, S. S. Iyengar, J. Tomasi, M. Cossi, N. Rega, J. M. Millam, M. Klene, J. E. Knox, J. B. Cross, V. Bakken, C. Adamo, J. Jaramillo, R. Gomperts, R. E. Stratmann, O. Yazyev, A. J. Austin, R. Cammi, C. Pomelli, J. W. Ochterski, R. L. Martin, K. Morokuma, V. G. Zakrzewski, G. A. Voth, P. Salvador, J. J. Dannenberg, S. Dapprich, A. D. Daniels, Ö. Farkas, J. B. Foresman, J. V. Ortiz, J. Cioslowski, and D. J. Fox, Gaussian, Inc., Wallingford CT, 2009.

Preference for Propellane motif in Pure Silicon Nanosheets

S. Marutheesswaran[a], Pattath D. Pancharatna[a] and Musiri M. Balakrishnarajan[*a]

Entry for Table of Contents

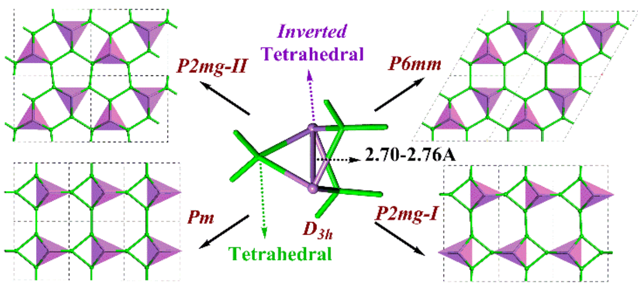

Two-dimensional nanosystems of pure silicon energetically prefer nonclassical propellane structure as the basic building block over sp^2-hybridized silicene. All the isomeric forms are found to be semiconductors with a narrow band gap.